ABSTRACT

GUIDANCE CONTROL OF SMALL UAV WITH ENERGY AND MANEUVERABILITY LIMITATIONS FOR A SEARCH AND COVERAGE MISSION

By

German G. Gramajo

August 2014

This thesis presents an algorithm for a search and coverage mission that has increased autonomy in generating an ideal trajectory while explicitly considering the available energy in the optimization. Further, current algorithms used to generate trajectories depend on the operator providing a discrete set of turning rate requirements to obtain an optimal solution. This work proposes an additional modification to the algorithm so that it optimizes the trajectory for a range of turning rates instead of a discrete set of turning rates. This thesis conducts an evaluation of the algorithm with variation in turn duration, entry-heading angle, and entry point. Comparative studies of the algorithm with existing method indicates improved autonomy in choosing the optimization parameters while producing trajectories with better coverage area and closer final distance to the desired terminal point.

GUIDANCE CONTROL OF SMALL UAV WITH ENERGY AND MANEUVERABILITY LIMITATIONS FOR A SEARCH AND COVERAGE MISSION

A THESIS

Presented to the Department of Mechanical and Aerospace Engineering

California State University, Long Beach

In Partial Fulfillment

of the Requirements for the Degree

Master of Science in Aerospace Engineering

Committee Members:
Praveen Shankar, Ph.D.
Jalal Torabzadeh, Ph.D.
Panadda Marayong, Ph.D.

College Designee:

Antonella Sciortino, Ph.D.

By German G. Gramajo

B.S. in Aerospace Engineering, 2011, California State Polytechnic University, Pomona

August 2014

ProQuest LLC.
789 East Eisenhower Parkway
P.O. Box 1346
Ann Arbor, MI 48106 - 1346

ACKNOWLEDGEMENT

I would like to thank my advisor, Dr. Praveen Shankar, for the advice and assistance he has provided me these past years. His support has made this thesis possible. I would also like to thank my review committee, Dr. Jalal Torabzadeh, Dr. Bei Lu, and Dr. Panadda Marayong, for taking the time to review and provide comments on this thesis. Lastly, I would like to thank my parents, Abigail and Maritza Gramajo, for all their support and unconditional love throughout my life. Without their courage to set out in their journey to the United States, leaving their war torn country, I would not have had this privilege of acquiring a college education and reaching this point in my life. More importantly, their journey through the desert to reach the United States has been my inspiration for my own desert journey.

TABLE OF CONTENTS

Page

CHAPTER Page

LIST OF TABLES

TABLE Page

TABLE Page

LIST OF FIGURES

FIGURE Page

NOMENCLATURE

A( )	New area covered function
C( )	Terminal cost function
D	Drag
S( )	Priority Function
S	Wing Area
K	Number of turn during the mission for the energy available
W	Discrete set of turning rates
X	Location of vehicle in Cartesian coordinates
AR	Wing aspect ratio
C_{D_0}	Zero-lift drag coefficient
E_{total}	Total Energy
$E_{consumed}$	Energy Consumed
$P_{required}$	Power required for steady level flight
P_{traj}	Power required for the possible trajectories
X^{exit}	Exit location in Cartesian coordinates
e	Oswald's efficiency factor
g	Gravity
m	Mass of vehicle
n	Load factor
v	Velocity

$\overline{x}$	x component of distance from the location of the vehicle to the center of uncovered area
$\overline{y}$	y component of distance from the location of the vehicle to the center of uncovered area
t_{exit}	Time to reach the exit state assuming straight path from location at end of time step
t^{exit}	Allocated end time of the mission
t_{safe}	Time to safely reach the exit point from the location of the vehicle
Ψ	Sensor footprint Area
Ω	Area not covered yet
ρ	Air density
τ	Turn duration also referred to as sampling time
ω	Turning Rate
$\dot{\theta}_{max}$	Maximum turning rate bounding the range turning rates

CHAPTER 1

INTRODUCTION

Recent improvements and development of small autonomous aerial vehicles has made them very inexpensive and valuable tool for civilian and military use. Small inexpensive autonomous aerial vehicles are of great interest in military and civilian application for missions such as search and coverage, surveillance, surveying, border patrol, and mapping missions [1, 2]. These missions are the type of mission that are time critical or require a repetitive action, in order to find objects/targets as soon as possible or to generate a collage of an area, which is the reason for the desired use of small-unmanned aerial vehicles in these types of missions. The small-unmanned aerial vehicles allow for faster covering of an area, without increasing human risk, and reducing cost [1, 2]. One of the challenges is planning the path for the coverage problem.

1.1 Purpose

The intention of this thesis is to develop a highly autonomous algorithm that generates a trajectory to maximize the spatial coverage of a specified region given a constraint on the available energy, while still satisfying the original flight plan of reaching the desired exit point. The goal of the proposed algorithm is to generate a trajectory that covers the most area and approach the exit point as much as possible for any selected value of the variables, for trajectories within a range of turning rates, and energy available.

One of the challenges is developing an algorithm that generates a near optimal trajectory for any of the following conditions: turn duration, entry-heading angle, and entry-point. Therefore, the fundamental goal of this thesis is to develop an algorithm with high autonomy such that the algorithm generates an optimal trajectory possible for any conditions provided by the operator. An algorithm with low autonomy requires the operator to provide the appropriate conditions to generate the trajectory with optimal performance, leading to the need of simulation of several test cases. A high level of autonomy eliminates the need to spend time in simulations to obtain the correct combination of conditions that generates the optimal trajectory, allowing the operator to deploy the vehicle in any configuration without having to verify that the algorithm will generate near optimal trajectories.

Other challenges include developing a cost function that considers the amount of energy available and the amount of energy consumed in order to select a trajectory in future time steps. The cost function depends on modeling the power consumption of the vehicle to perform a particular maneuver by calculating the amount of energy required by the vehicle to maintain a constant velocity for the turn rate of the maneuver. In addition, the cost function keeps track of the energy remaining. This allows the vehicle to know of the path that it can actually perform and still finish near the exit state.

Although, the thesis presents an algorithm to generate a trajectory that maximizes the spatial coverage for a vehicle with energy limitations, the motivation of the work presented is to implement the algorithm in a cooperative search and coverage mission for vehicles with heterogeneous task. The intention is to use the algorithm presented in this

thesis on a search vehicle that will be cooperating with a secondary vehicle, operating in the same area. The second vehicle will be investigating points of interest identified by the search vehicle. The search vehicle has to cover the specified region while avoiding collision with the secondary vehicle. As previously stated, this thesis primarily focuses on the algorithm for the search vehicle that has to cover the most area possible and reach the exit state for the energy available.

1.2 Background/Related Work

The coverage path-planning problem occurs in many applications and is not limited to only unmanned aerial vehicles. The problem frequently occurs in many day-to-day applications of general robots performing a repetitive task requiring the robot to cover an area. The literature review includes work done on robots used in everyday tasks such as lawn mowing, vacuuming, and plowing since the motion of the vehicle resembles the two-dimensional plane motion of robots performing floor coverage of the mentioned tasks [3, 4]. Since the problem occurs in many applications, an extensive amount of literature dealing with the coverage path-planning problem exists, leading to several solutions. Provided below is a brief literature review of path planning and coverage. As previously stated, the works include coverage path planning for general robots specifically for unmanned aerial vehicle coverage path planning.

One of the methods used in path planning for coverage utilizes the principle of boustrophedon motion [3, 4, 5, 6, 7, 8]. Boustrophedon decomposition is a method in which the space that the robot has to cover is broken down into cells that are covered in back and forth boustrophedon motion. The method of planning the path guarantees

complete coverage of a specified region but it is not adequate for the intended mission. Since the method does not consider a mission duration, exit point, or energy available. The method is just concerned with generating a path that covers all points inside the specified region. The method focuses on generating a trajectory that accomplishes complete coverage and does not have any other task or consider that the vehicle may not be able to complete the generated trajectory due to energy limitations. More importantly, the set pattern used to cover the area is not practical scenario of covering the specified region for the intended mission since it creates a conflict for the search vehicle of maintaining the boustrophedon motion and avoiding the secondary vehicle.

Other methods reviewed in this thesis included the utilization of rapidly exploring-random tree path planner [5, 9]. The planner generates random path and the randomness makes the results not fully satisfactory. This approach of generating a path has limitations with the slow response. Since the path generation is random and does not have to follow set waypoints determined before starting the mission, this method is practical for the intended mission because the vehicle does not have a conflict of interest in maintaining a set pattern to cover an area and avoid collision with any other vehicles operating in the same area. However, this method like the one previously mentioned does not serve the purpose of the intended mission since it does not optimize the generated trajectory for the energy available or an exit point.

A method for path planning proposed by Balakrishnan [10] considers a discrete space of the specified region. By discretizing the space, the vehicle generates a network of point previously covered and point still not covered. The primary focus of this method

is to generate a path that covers all the discrete points inside the region. The method does not worry about optimizing the path so that it reaches an exit state after a certain time of before running out of energy. The method works by selecting neighboring point, not previous covered, from the location of the vehicle. This method does not work for the intended mission for several reasons. One of the reasons that it does not work is because it can generate trajectories with ninety-degree turns. Another reason that the discrete space does not work because the discrete points are waypoints that the vehicle has to visit throughout the mission and the intended mission does not require any waypoints for the vehicle to visit as it performs the mission. As in the previous method discussed, this approach purely focuses on covering all the area since it does not consider whether the vehicle can complete the entire generated trajectory. This method is very similar to the proposed method of path planning using grid coverage trajectory planning [11]. In the method, the path generated is for region discretized into a grid providing the point that the robot has to pass in order to cover the entire region. However, this method considers the battery voltage constraint, which provides an idea on the way to implement the energy constraint in the algorithm so it that it optimizes for the energy available.

Several other methods reviewed utilize the knowledge of the region as an input to the path-planning algorithm. These methods rely on the operator knowing beforehand the possible location of objects/targets that he/she is searching for in a specified region and generates a probability map of the specified region. These methods of generating a path to search and cover a region are greedy heuristics (probabilistic search) and potential based heuristics [12, 13]. In the greedy heuristic, the algorithm generates the path by

moving to neighboring cells that have the highest probability of containing an object/target. In the potential based heuristics, the algorithm selects the path by calculating the attraction and repulsive potentials for goals and obstacles, respectively.

Previous and related work also includes path generation for multiple vehicles searching and covering an area. The proposed methods in generating a path for a search and coverage mission by Polycarpous, Yang, and Passino [14] and Kumar [15] rely on an algorithm that minimizes the amount of area uncovered. Polycarpous et al. provides a very general framework of the algorithm that generates the path that will cover the specified region for several possible paths, using an on-line architecture [14]. Using Polycarpous et al.'s method to generate the path relies on search maps of the area covered and the area not yet covered [14]. Given the updated information of the search maps and the knowledge of the possible path, the selection of the search path depends on the multi-objective cost function. On the other hand, Kumar's approach generate a trajectory for a discrete set of turning rates optimizing the trajectory so that it covers the most area possible and reaches the exit point at the allocated mission time [15]. This approach depends on discretizing the region in order to calculate the area covered by the possible path for the discrete set of turning rates. The algorithm selects a trajectory that covers more area as long as the cost function determines that that sufficient mission time remains for the vehicle to continue covering and reach the exit point. As the remaining time reduces, the cost function determines the path that takes the vehicle directly to the desired exit point at the end of the mission duration.

The algorithms proposed by Polycarpous et al. and Kumar, specially Kumar's algorithm, are the foundation of the algorithm proposed in this thesis since they perform the required task of the intended mission of covering a region and reaching a desired exit state. Kumar's approach of generating the trajectory that covers and approaches an exit point is practical for the intended mission since the path is not restricted to a particular path pattern, so the algorithm can easily generate a path that will avoid collision with other vehicles operating in the same area. Even though, the algorithm does not consider the energy constraint in optimizing the generated trajectory, modification of the cost function in Kumar's algorithm are possible so that it considers the energy constraint when optimizing the trajectory. However, Kumar's algorithm has several deficiencies such as limited autonomy since it only generates near optimal trajectories for particular conditions that the operator has to select.

CHAPTER 2

DESIGN AND IMPLEMENTATION OF PATH PLANNING ALGORITHM

The motivation is to develop an algorithm that generates a trajectory in real-time to maximize the coverage of a specified region while maintaining its original flight plan of reaching set exit point at the end of the mission for set amount of energy and conditions. Figure 1 demonstrates a visual representation of the problem of generating a trajectory that maximizes the area covered and satisfies the exit stated for energy available. Figure 2 demonstrates the generated trajectory along with the sensor footprint area throughout the mission. Kumar proposed an algorithm that generates off-line trajectories that maximizes the spatial-temporal coverage while still satisfying it original flight plan of reaching a set exit point at the end of the mission but for a set amount of time [15]. The proposed algorithm by Kumar is a receding horizon control algorithm optimizing the trajectory for a discrete set of turning rates and a time constraint. Kumar's algorithm is the foundation of the proposed algorithm in this thesis since it performs the desired task. As previously stated, Kumar's algorithm generates the trajectories off-line and for a time constraint instead of in real-time and for an energy constraint, so this thesis transforms Kumar's algorithm from an off-line time constraint trajectory optimization into a real-time energy constraint trajectory optimization. However, the algorithm proposed by Kumar has several deficiencies that this thesis addresses in order to improve

the functionality of the algorithm and make the algorithm more autonomous in generating the trajectories.

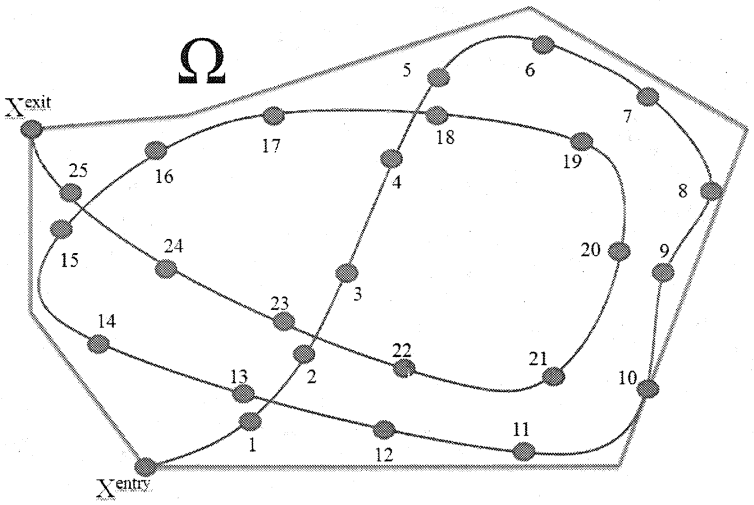

FIGURE 1. Problem of generating a trajectory that maximizes the area covered while satisfying the exit state for the energy available.

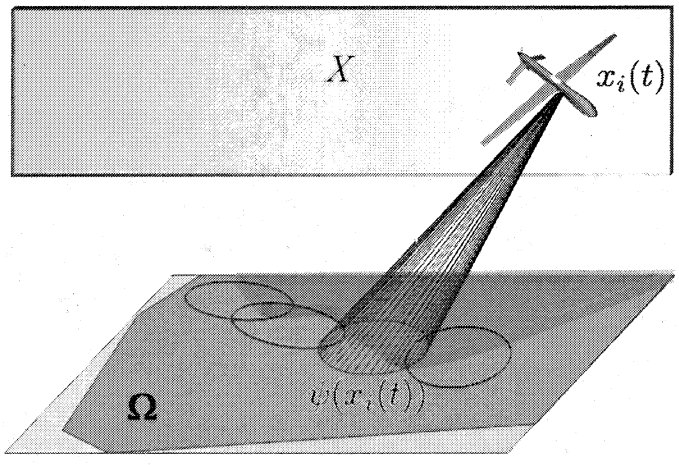

FIGURE 2. Area covered by sensor footprint for generated trajectory throughout the mission.

2.1 Receding Horizon Control Algorithm for a Discrete Set of Turning Rates with a Time Constraint

This section provides a brief description of the algorithm that is the foundation of the proposed algorithm in this thesis. As previously stated, the foundation of the proposed algorithm is a receding horizon control algorithm optimizing the trajectory for a discrete set of turning rates and a time constraint. The algorithm generates the trajectory off-line before the vehicle begins the mission and it generates the trajectory for multiple vehicles performing the same task. The algorithm is a minimization function of the sum of the uncovered area and the cost function. The cost function calculates the cost of the vehicle to reach the desired exit point at the end of the mission duration for the location of the vehicle at the end of the turn duration, denoted by τ.

$$\begin{aligned} &\min_{[W_1,\ldots,W_n]}\left[\text{area}\left(\Omega(k-1) - \cup_n \psi_n\left(X_n(t)\right)\right)\right] + \textstyle\sum_n C\left(X_n\left((k+1)\tau\right), X_n{}^{exit}, t_n{}^{exit}\right) \\ &X_n(k\tau) = X_n^{exit}((k-1)\tau \\ &\left\|X_i(t) - X_j(t)\right\| > d_{safe} \end{aligned} \quad (1)$$

Equation 1 provides the receding horizon control based algorithm with a time constraint and discrete set of turning rates for the time period $[k\tau, (k+1)\tau]$ for k=m, 1,…, q. The variables m and q are $t^{entry}=m\tau$ and $t^{exit}=q\tau$, respectively. Equation 1 is an algorithm for multiple vehicles searching an area generating the trajectory for a discrete time period $[k\tau, (k+1)\tau]$. W denotes the discrete set of turning rates for the vehicle. $\Omega(k-1)$ is the area not yet covered and $\Omega(m)$ equals the area of the specified region. The variable $\psi(X(t))$ denotes the sensor footprint area at time t.

The function C is the terminal cost function at time t, which determines the optimal trajectory for the vehicle to take to reach the exit point for the remaining mission time left. Equation 2 provides the definition of the terminal cost function. The cost

function determines the objective of the vehicle according to the value of the cost function. If the vehicle has enough time, the cost function is set to zero and the vehicle's objective is to cover the most area possible, but as the remaining time reduces the objective changes from coverage to going directly to the exit point. In equation 2, T(X(t), X^{exit}) is the minimum time of travel to the exit point assuming that the vehicle uses a straight path to the exit point. The variable t_{safe}, t, and t^{exit} are the time of the minimum collision free trajectory to the final state, the time elapsed, and the time at the end of the mission, respectively.

$$C(X_n(t), X_n{}^{exit}, t_n{}^{exit}) = \begin{cases} 0 & \text{if } \left(t_n{}^{exit} - \left((t + T_n(X_n(t), X_n{}^{exit})\right)\right) > t_{safe} \\ \frac{1}{t_n{}^{exit} - \left(t + T_n(X_n(t), X_n{}^{exit})\right) + \varepsilon} & \text{if } 0 \le \left(t_n{}^{exit} - \left(t + T_n(X_n(t), X_n{}^{exit})\right)\right) \le t_{safe} \\ \infty & \text{if } \left(t_n{}^{exit} - \left(t + T_n(X_n(t), X_n{}^{exit})\right)\right) < 0 \end{cases} \quad (2)$$

Equation 1 generates the trajectory by selecting from the possible path for the discrete set of turning rates the trajectory with the lowest sum of the area and terminal cost function. Once the algorithm selected the path with the lowest sum, it feedback the final position of the selected trajectory for the turn duration and generates the path for the following time step. The results using the current in equation 1 are in Tables 1 through 7. The results demonstrate the deficiencies of the existing algorithm. The following section addresses the deficiencies of the algorithm and improves them in order to improve the performance of the algorithm.

2.2 Receding Horizon Control Algorithm Optimizing the Trajectory for a Range of Turning Rates and Time Constraint

This section addresses the deficiencies of the previously discussed algorithm and provides improvement to deal with the deficiencies. As stated in the previous section the

existing algorithm generates the trajectory that maximizes coverage and reaches the exit point for a set of discrete turning rates. Generating the trajectories for a discrete set of turning rates makes the algorithm obtain only the optimal trajectory for the discrete set of turning rates instead of garneting the most optimal trajectory. In addition, generating the trajectory for a discrete set of turning rates make the algorithm dependent on the operator to select the correct combination of turning rates for the set of turning rates that will generate near optimal trajectories. If the operator selects the wrong combination of turning rates, the algorithm generates a trajectory with a highly degraded percentage of the region covered and an end of trajectory far from the desired exit state. However, obtaining the optimal set of turning rates is very tedious and time consuming because it requires trial and error of all possible combinations of the turning rates. Even after investing the time and effort to find the absolute optimal set of turning rate for a set of conditions, the set of turning rates obtained is not the absolute optimal set of turning rates for different conditions such as different selected turn duration, entry-heading angle, and entry point.

The algorithm proposed in this section improves the stated deficiencies by increasing the autonomy of the algorithm in generating the optimal trajectory. The algorithm has an increased autonomy since it will not depend on the operator providing the correct set of turning rates, turn duration, entry-heading angle, and entry. Therefore, the expectation of the proposed algorithm is to generate the most optimal trajectory possible for any given set of conditions. Equation 3 is the proposed algorithm meant to improve the deficiencies of the existing algorithm, which selects the trajectory with the

lowest value. Equation 3 presents the proposed algorithm for the time period $[(k-1)\tau, k\tau]$ for k=1,2,…,K in which K is the amount of turns during the mission for the amount of energy available. Since the number of turn that the vehicle will perform during the mission for the energy available and conditions is uncertain until the vehicle performs the mission, the value of K at the beginning of the mission is unavailable so the amount of time steps required to generate the trajectory is uncertain. $\Omega((k-1)\tau)$ is the area not yet covered and $\Omega(0)$ is the area uncovered at the beginning of the mission, which is the area of the specified region .

$$\min_{[-\dot{\theta}_{max}<\omega<\dot{\theta}_{max}]}\left[S(X(t), X^{exit}, t^{exit})A\left(X(k\tau), \Omega\left((k-1)\tau\right)\right)\right] + C(X(k\tau), X^{exit}, t^{exit}) \qquad (3)$$

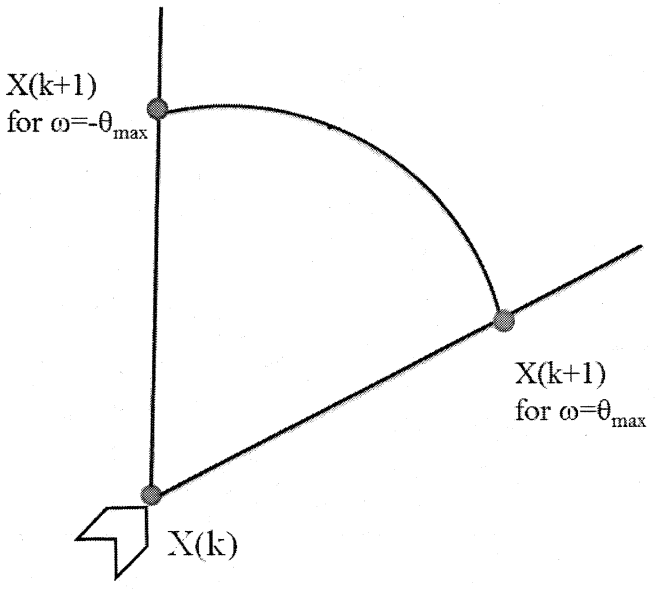

FIGURE 3. Selection of the next point in the path of the vehicle for a range of turning rates.

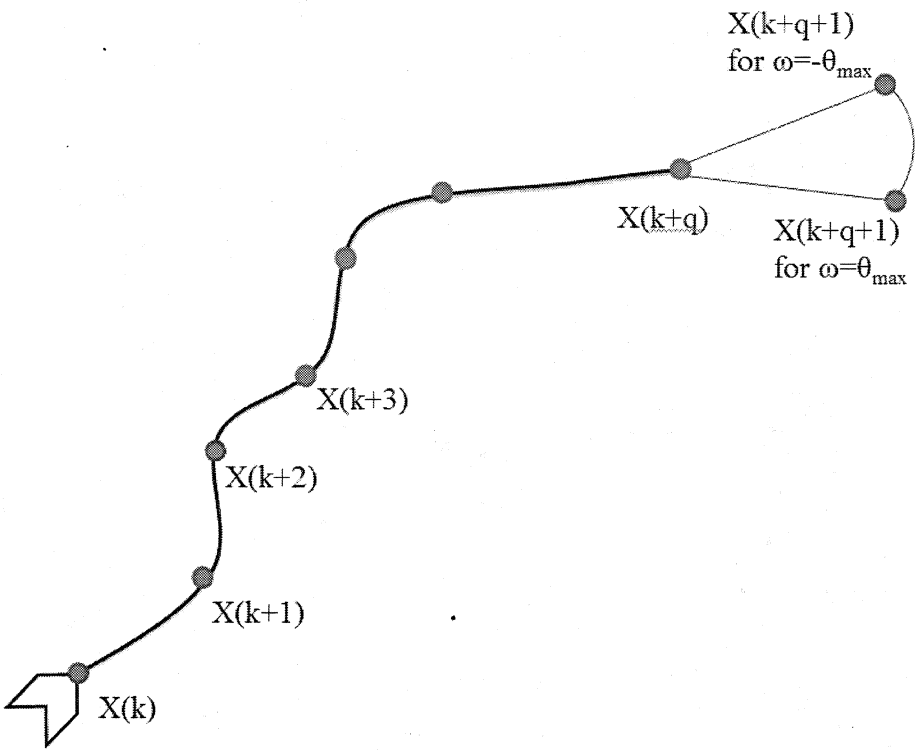

FIGURE 4. Trajectory generated using the receding horizon control algorithm that optimizes the trajectory for a range of turning rates.

In order to replace the requirement for a discrete set of turning rates provided by the operator, the proposed algorithm suggests optimizing the trajectory for a range of turning rates instead. By optimizing the trajectory for a range of turning rates instead of a discrete set of turning rates eliminates requirement of the operator providing the correct set of turning rates. Similarly, the receding horizon control based algorithm's dependence on the operator providing the appropriate turn duration, entry-heading angle, and entry-point to generate a near optimal trajectory, the proposed algorithm replaces the area portion of the previous algorithm with a new area covered function alongside apriority function. The new area covered function calculates the new area covered by the

possible trajectories generated for the turning rates within the turning rate range. The priority function determines the objective of the vehicle as it generates the path of either covering the most area possible or heading straight to the exit state.

Equation 4 provides in detail the new area covered function proposed in this thesis meant to improve the deficiency of the existing algorithm requiring particular conditions in order to produce near optimal trajectories. $\Psi(X(k\tau)$ is the sensor footprint for the path up until coordinate point $X(k\tau)$ and $\Omega((k\text{-}1)\tau)$ is the area not yet covered at time $(k\text{-}1)\tau$. The new area covered function determines if the trajectory covers new area, if new area is covered then the new area covered function is equal to the inverse of the new area covered. However, if the trajectory does not cover any new area then the function is equal to the distance from the end of the trajectory for the current time step to the center of the uncovered area. The conditions of the new area covered function enable the algorithm to generate optimal trajectories for any selected turn duration since it directs the trajectory to area not previously covered when the generated trajectories for the turn duration go outside the boundaries of the specified region or stay within previously covered area. The previous algorithm was not adaptive enough to direct the vehicle towards area not previously covered when the generated trajectory stayed within previously covered area or went outside the boundaries of the region for the selected turn duration.

$$A\left(X(k\tau), \Omega\left((k-1)\tau\right)\right) = \begin{cases} \frac{1}{\psi_1(X(k\tau)) \cap \Omega((k-1)\tau)} & \text{if } \psi_1\left(X_1(k\tau)\right) \cap \Omega(k-1) > 0 \\ \sqrt{\bar{x}^2 + \bar{y}^2} & \text{if } \psi_1\left(X_1(k\tau)\right) \cap \Omega(k-1) = 0 \end{cases} \quad (4)$$

In addition, the priority function improves the receding horizon control based algorithm with a time constraint for a discrete set of turning rates by determining when to use equation 4 to generate the most optimal coverage trajectory possible. As previously stated, the priority function determines the objective of the vehicle for generating the trajectory. Equation 5 provides the piecewise function that defines the priority function to determine the objective of the vehicle. Equation 5 gives priority to covering the most area possible when enough time remains by setting the priority function equal to one and when not enough time remains the priority function is equal to zero giving priority to going directly to the exit state. This definition of the priority function guarantees that there will not be any conflict of interest between covering and going directly to the exit state when not enough time remains. The definition of the priority function makes the algorithm neglect the value of the trajectories to cover new area when the remaining time is low, so the algorithm just focuses on the terminal cost to reach the exit state when insufficient time remains for vehicle to continue covering the specified region.

$$S(X(t), X^{exit}, t^{exit}) = \begin{cases} 1 & if \left(t_n{}^{exit} - \left((t + T_n(X_n(t), X_n{}^{exit})\right)\right) > t_{safe} \\ 0 & if \ 0 \le \left(t_n{}^{exit} - \left(t + T_n(X_n(t), X_n{}^{exit})\right)\right) \le t_{safe} \\ 0 & if \ \left(t_n{}^{exit} - \left(t + T_n(X_n(t), X_n{}^{exit})\right)\right) < 0 \end{cases} \quad (5)$$

2.3 Receding Horizon Control Algorithm Optimizing the Trajectory for a Range of Turn Rates and Energy Constraint

This section addresses the trajectory generation for a search and coverage mission that maximizes the coverage while satisfying the final state for the energy constraint of the vehicle and the maneuverability limitation. The receding horizon control based algorithm without energy constraint for a discrete set of turning rates generates the

optimal trajectory that maximized coverage while satisfying the exit state for the mission time constraint [15]. The receding horizon control based algorithm without energy constraint method of generating the trajectory for the mission time constraint is an inefficient method of generating the trajectory. Neglecting the energy constraint in generating the trajectory results in the vehicle executing a trajectory not optimized for the energy available, a trajectory that the vehicle may not be able to complete for the available energy. The vehicle does not satisfy the exit state and consumes the total energy available before the mission duration for trajectory optimized for the mission duration. The vehicle consumes the total energy before the allocated mission duration for a trajectory optimized for the mission duration since the generated trajectory assumes that the vehicle consumes the energy at a constant rate. In reality, the vehicle does not consume the energy at a constant rate in a search and coverage mission because such mission is not a steady level flight. For a search and coverage mission the vehicle has to perform maneuvers and the energy consumption of a vehicle varies for different maneuvers. Therefore, considering the energy constraint to generate the optimal coverage trajectory ensures that the vehicle satisfies in approaching the exit state as much as possible for the total energy available since the algorithm optimizes the trajectory for the available energy.

$$\min_{-\omega_{max}<\dot{\theta}<\omega_{max}} \left[S(X(k\tau), X^{exit}, E_{total}, E_{consumed})A\left(X(k\tau), \Omega((k-1)\tau)\right) + C(X(k\tau), X^{exit}, E_{total}, E_{consumed})\right] \quad (6)$$

Equation 6 represents the optimization for the proposed algorithm that generates the trajectory with energy constraint. The algorithm includes the improvements to the

algorithm addressed in the previous section, so that the algorithm generates the most optimal trajectory possible for any provided condition of turn duration, entry-heading angle, and entry point. Equation 6 uses the same new area covered function used in equation 3 ad also optimizes the trajectory for a range of turning rates. The modification made to equation 3 to obtain equation 6 mainly involved a terminal cost function that considers the energy constraint instead of the time constraint. The condition of the priority function stated in equation 5 change also well since the conditions of the priority function have to coincide with conditions of the terminal cost function, which now will have conditions for the energy constraint.

As previously stated the algorithm generates the optimal coverage trajectory for a vehicle with energy and maneuverability limitations. This section first addresses the maneuverability limitations of the vehicle for the algorithm presented in equation 6. The algorithm considers the maneuverability limitations of the vehicle by optimizing the trajectory for a range of turning rates, in which the bounds of the turning rate range are the maximum turning rates that the vehicle can achieve. The maximum turning rate of the vehicle that defines the range of turning rates derives from the maximum loading factor that vehicle can achieve when it performs a maneuver. Equation 7 defines the maximum turning rate of the vehicle for the maximum loading factor of the vehicle. Anderson and Raymer provide the relationship between loading factor and turning rate used in equation 7 [16, 17]. Therefore, the algorithm only generates trajectories within the range of admissible turning rates, ensuring that the algorithm does not exceed the maneuverability capabilities of the vehicle.

$$\omega_{max} = \frac{g\sqrt{n_{max}{}^2 - 1}}{v} \tag{7}$$

Next, the section addresses the terminal cost function considering the energy constraint instead of the time constraint. Equation 8 defines terminal cost function with the energy constraint that makes the algorithm in equation 6 generate the most optimal trajectory for the energy available. The terminal cost function in equation 8 is similar as the terminal cost function defined in equation 2, with the only difference that it selects the trajectory for the energy remaining instead of the time remaining. Therefore, the terminal cost function in equation 8 examines the amount of energy required by the vehicle to reach the exit state, denoted by X^{exit}, from the path's end at each time step and compares it to the remaining energy. The energy required to reach the exit state from the possible path's ends at each time step assumes that the power required and time to travel is for the vehicle using a straight path to the exit point denoted by $P_{required}$ and t_{exit}, respectively. The cost is set to zero when enough energy remains for the vehicle to continue covering the region, in which case, the objective is to cover as much area as possible, and when enough energy does not remain the objective is to go directly to the exit state.

$$C\left(X(k\tau), X^{exit}, E_{total}, E_{consumed}(t)\right) =$$

$$\begin{cases} 0 & \text{if } E_{total} - \left(E_{consumed}(t) + P_{traj}(\dot{\theta})\tau\right) > P_{required} t_{exit} \\ \frac{1}{E_{total} - \left(E_{consumed}(t) + P_{traj}(\dot{\theta})\tau\right)} & \text{if } 0 \le E_{total} - \left(E_{consumed}(t) + P_{traj}(\dot{\theta})\tau\right) \le P_{required} t_{exit} \\ \infty & \text{if } E_{total} - \left(E_{consumed}(t) + P_{traj}(\dot{\theta})\tau\right) < 0 \end{cases} \tag{8}$$

$P_{required}$ is the power required by the vehicle flying in steady level flight and t_{exit} is the time to reach the exit state using the straight path for the constant velocity of the vehicle. Equation 9 and 10 provide the power required for steady level flight and the

time to reach the exit state from the path's end at each time step, respectively. Equation 9 is the minimum power required by the vehicle in steady level flight for the vehicle's specifications at a set altitude. Multiplying the values of equation 9 and 10, as done in equation 8 for the conditions of the piecewise function, results in the calculated energy required for the vehicle to reach the exit state. Anderson and Raymer provide the equation of minimum power required of a vehicle in a steady level flight for the vehicle's specifications used in equation 9 [16, 17].

$$P_{required} = vD = v\left(\frac{1}{2}\rho v^2 S C_{D_0} + \frac{4(mg)^2}{\rho v^2 S \pi A R e}\right) \tag{9}$$

$$t_{exit} = \frac{\sqrt{\left(X((k+1)\tau) - X^{exit}\right)^2}}{\dot{} \; v} \tag{10}$$

Generation of the optimal trajectory of the vehicle requires comparing the calculated energy required by the vehicle to reach the exit state with the energy remaining at the possible locations of the vehicle at the end of a time step. To obtain the energy remaining at the possible locations at the end of a time step requires calculating the power required for the possible trajectories from the range of turning rates, denoted by P_{traj} in equation 8. Equation 11 defines P_{traj} the power requirements of a possible trajectory for the load factor of the turn rate. Equation 12 provides the load for a turn rate for the vehicle at a constant velocity.

$$P_{traj} = vD = \dot{v}\left(\frac{1}{2}\rho v^2 S C_{D_0} + \frac{4(mg)^2 n^2}{\rho v^2 S \pi A R e}\right) \tag{11}$$

$$n = \sqrt{\left(\frac{\dot{\theta}v}{g}\right)^2 + 1} \tag{12}$$

The conditions of the priority function have to coincide with the conditions of the terminal cost function so that algorithm depends only on the new area covered function when enough energy remains for the vehicle to continue covering the region and on the terminal cost function when little energy remains. Modifying equation 5 so that the conditions coincide with the conditions of equation 8 produces equation 13.

$$S(X(t), X^{exit}, t^{exit}) = \begin{cases} 1 & \text{if } E_{total} - (E_{consumed}(t) + P_{traj}(\dot{\theta})\tau) > P_{required}t_{exit} \\ 0 & \text{if } 0 \le E_{total} - (E_{consumed}(t) + P_{traj}(\dot{\theta})\tau) \le P_{required}t_{exit} \\ 0 & \text{if } E_{total} - (E_{consumed}(t) + P_{traj}(\dot{\theta})\tau) < 0 \end{cases} \tag{13}$$

CHAPTER 3

RESULT AND DISCUSSION

The motivation of the thesis is to be able to implement the proposed algorithm in this thesis in real-time and generate optimal coverage trajectories for any determined condition of turn duration, entry-heading angle, and entry point. The results in this chapter include the performance of the receding horizon control based algorithm without an energy constraint for a discrete set of turning rates, proposed by Kumar [15], in generating an optimal coverage trajectory, for determined conditions. The algorithm by Kumar is the foundation of the proposed algorithm in this thesis. The results present the performance of the receding horizon control based algorithm without the energy constraint for a discrete set of turning rates in generating an optimal trajectory in order to compare the performance with the proposed modified algorithm of this thesis and demonstrate that the proposed modified algorithm improves in the deficiencies of the existing algorithm. In addition, the results include the performance of the proposed modified algorithm in this thesis implemented in real-time in the presence of an uncertainty in the actual position of the vehicle and the planned position at the end of each sampling time. Lastly, the results include the performance of the proposed algorithm that optimizes the trajectory for the energy constraint and compares it to the performance of the algorithm that generates the optimal trajectory without considering the energy constraint.

The assumption made is that the vehicle is moving in a two-dimensional plane operating at a constant altitude of 400 meters. The vehicle assumed in the simulation is a small-unmanned aerial vehicle of 5 kilograms, with a wing aspect ratio of 2, wing span of 1 meter, and zero-lift drag coefficient of .32. For the case that generates the trajectory for the time constraint the model used to perform the simulation assumes the vehicle operating at constant velocity of 11.49 meters per second, searching a region of 559 meters by 559 meters, exit point of p^{exit}=[10, 569], and a mission duration time of 9 minutes. For the case of optimizing the trajectory for the energy constraint, the parameters are the same except the flight time replaced with a total energy of 87912 Joules for a battery of 2200 mAh and 11.1 volts. In addition, the model for cases of the trajectory optimization for the energy constraint assumes a maximum load factor of 1.5, which results in a turning rate range bounded by -.9548 and .9548 rad/s.

3.1 Simulation Results of Receding Horizon Control Algorithm Optimizing Trajectory for a Discrete Set of Turning Rates and Time Constraint

The purpose of implementing the existing algorithm proposed by Kumar was to determine and improve its deficiencies and increase the autonomy of the algorithm in generating the optimal trajectories for any set conditions. The presented results verify that the modified algorithm improves the performance of the existing algorithm for any determined value of the turn duration, entry-heading angle, and entry point variables. Using the existing algorithm requires a discrete set of turning rates to generate the optimal trajectory that maximizes spatial-temporal coverage while satisfying the initial flight plan of reaching the final position at the end of the mission. The results demonstrate the amount effort required to obtain one possible set of optimal set of turn

rates. In addition, the presented results are for varying turn duration, entry-heading angle, and entry point for a discrete set of turning rates. For instance, the results demonstrate the effects in the selection of the stated variables on the generated trajectories on the degradation of the percent of area covered and a greater distance from the exit point at eh end of the mission. Tables 1 through 6 provide the results generated using the existing algorithm.

3.1.1 Discrete Set of Turning Rates

This section demonstrates the amount of effort required to obtain the best set of turning rates for a set of conditions that maximize the area covered and satisfies the exit point at the end of the mission. In order to obtain the best set of turn rates that achieved the maximum coverage and satisfy the exit states requires testing all the possible combinations of turn rates and iteratively increasing the number of turn rates. Continue increasing the number of turn rates until the percent of area covered stops increasing and the distance of the vehicle from the exit states stops reducing. Increasing the number of turn rates eventually make the percent of area covered and the distance from the exit point converge, but as the number of turn rates increase the amount of computations and time to generate a trajectory. Tables 1, 2, and 3 provide simulation results of possible turn rate combinations for sets of 3, 5 and 7 turn rates, respectively.

Table 1 provides the percent of the region covered and the distance from the exit point for a sampling time (the turn duration) of 10 seconds, an entry point p^{entry}=[10 ,10], and entry-heading angle of 45 degrees. The generated results for Table 1 are for a discrete set of 3 possible turning rates including one trajectory for zero turning rate and

the remaining two are turning rates for one to each side. The table provides the best trajectory for the combination for a set of three turning rates. From Table 1, it is evident that the generated trajectory for turning rates 0, 0.23562, -0.23562 rad/s generates the best coverage trajectory but it is not the best trajectory in reaching the exit point, since other paths get nearer to the exit point at the end of the mission.

TABLE 1. Percent of Area Covered and Distance from Exit Point for Set of Three Turning Rates

Turn Rates (rad/s)	Percent Area Covered	Distance from Exit (m)
0, 0.00873, -0.00873	23.17	3005.97
0, 0.01745, -0.01745	23.60	160.51
0, 0.02618, -0.02618	35.75	616.14
0, 0.03491, -0.03491	23.60	696.44
0, 0.04363, -0.04363	26.04	508.75
0, 0.05236, -0.05236	52.00	201.19
0, 0.06109, -0.06109	29.43	183.83
0, 0.06981, -0.06981	30.99	194.98
0, 0.07854, -0.07854	41.85	102.90
0, 0.08727, -0.08727	34.22	140.30
0, 0.09599, -0.09599	29.46	146.18
0, 0.10472, -0.10472	63.07	144.54
0, 0.11345, -0.11345	32.01	35.17
0, 0.12217, -0.12217	39.74	101.92
0, 0.13090, -0.13090	34.24	37.48
0, 0.13963, -0.13963	45.55	120.54
0, 0.14835, -0.14835	93.47	57.52
0, 0.15708, -0.15708	92.93	44.11
0, 0.16581, -0.16581	89.09	53.13
0, 0.17453, -0.17453	77.59	79.08
0, 0.18326, -0.18326	73.82	83.96
0, 0.19199, -0.19199	89.39	111.08
0, 0.20071, -0.20071	92.74	82.15
0, 0.20944, -0.20944	80.31	50.53
0, 0.21817, -0.21817	86.61	18.73
0, 0.22689, -0.22689	92.91	104.66
0, 0.23562, -0.23562	95.23	89.49
0, 0.24435, -0.24435	69.74	110.17

TABLE 1. Continued Percent and Distance from Exit for a Set of Three Turning Rates

Turn Rates (rad/s)	Percent Area Covered	Distance from Exit (m)
0, 0.25307, -0.25307	51.61	56.94
0, 0.26180, -0.26180	83.01	71.46
0, 0.27053, -0.27053	91.19	60.88
0, 0.27925, -0.27925	90.66	68.91
0, 0.28798, -0.28798	74.52	104.43
0, 0.29671, -0.29671	79.82	7.25
0, 0.30543, -0.30543	92.23	65.12

The table presents the percent of the area covered and the distance from the desired exit point to the end of the trajectory for the sets of three turning rates. The parameters of the generated trajectories are a 10 second turn duration, entry point of [10, 10], entry-heading angle of 45 degree, desired exit point of (10,569), and a mission duration of 9 minutes.

TABLE 2. Percent of Area Covered and Distance from Exit Point for a Set of Five Turning Rates

Turn Rates (rad/sec)	Percent Area Covered	Distance from Exit (m)
0, 0.23562, -0.23562, 0.00873, -0.00873	89.96	22.83
0, 0.23562, -0.23562, 0.01745, -0.01745	94.42	90.31
0, 0.23562, -0.23562, 0.02618, -0.02618	93.70	106.17
0, 0.23562, -0.23562, 0.03491, -0.03491	91.03	96.16
0, 0.23562, -0.23562, 0.04363, -0.04363	95.81	54.98
0, 0.23562, -0.23562, 0.05236, -0.05236	82.21	108.70
0, 0.23562, -0.23562, 0.06109, -0.06109	83.72	89.78
0, 0.23562, -0.23562, 0.06981, -0.0698	84.73	22.25
0, 0.23562, -0.23562, 0.07854, -0.07854	92.75	103.34
0, 0.23562, -0.23562, 0.08727, -0.08727	94.30	77.01
0, 0.23562, -0.23562, 0.09599, -0.09599	97.71	27.88
0, 0.23562, -0.23562, 0.10472, -0.10472	84.19	32.67
0, 0.23562, -0.23562, 0.11345, -0.11345	77.43	93.25
0, 0.23562, -0.23562, 0.12217, -0.12217	94.70	14.50
0, 0.23562, -0.23562, 0.13090, -0.13090	96.27	70.57
0, 0.23562, -0.23562, 0.13963, -0.13963	95.94	32.80
0, 0.23562, -0.23562, 0.14835, -0.14835	69.63	117.41
0, 0.23562, -0.23562, 0.15708, -0.15708	60.05	110.11
0, 0.23562, -0.23562, 0.16581, -0.16581	77.61	2.51
0, 0.23562, -0.23562, 0.17453, -0.17453	86.80	99.51
0, 0.23562, -0.23562, 0.18326, -0.18326	79.83	13.05
0, 0.23562, -0.23562, 0.19199, -0.19199	55.99	24.73
0, 0.23562, -0.23562, 0.20071, -0.20071	85.83	22.14
0, 0.23562, -0.23562, 0.20944, -0.20944	89.76	60.63

TABLE 2. Continued Percent and Distance from Exit for a Set of Five Turning Rates

Turn Rates (rad/s)	Percent Area Covered	Distance from Exit (m)
0, 0.23562, -0.23562, 0.21817, -0.21817	70.78	45.72
0, 0.23562, -0.23562, 0.22689, -0.22689	95.38	100.81
0, 0.23562, -0.23562, 0.24435, -0.24435	81.30	58.70
0, 0.23562, -0.23562, 0.25307, -0.25307	87.21	21.04
0, 0.23562, -0.23562, 0.26180, -0.26180	79.47	56.04
0, 0.23562, -0.23562, 0.27053, -0.27053	83.48	106.50
0, 0.23562, -0.23562, 0.27925, -0.27925	96.21	48.23
0, 0.23562, -0.23562, 0.28798, -0.28798	94.47	44.28
0, 0.23562, -0.23562, 0.29671, -0.29671	70.82	82.56
0, 0.23562, -0.23562, 0.30543, -0.30543	90.15	89.57

The table provides the percent of the area covered and the distance from the desired exit point to the end of the trajectory for a set of five turning rates. The turning rates include the three best turning rates from Table 1. The parameters used to generate the trajectories are the same from Table 1.

Table 2 provides the percent of the region covered and distance from the exit point of the generated trajectory for the possible combinations of sets of five turning rates that includes the best set of turning rates from Table 1. As previously mentioned, the set of five turn rates used to generate the results in Table 2 includes the turning rates of 0, 0.23562, -.23562 rad/s, which is the best set of turning rates from Table 1. The generated results for Table 2 are for the same turn duration, entry point, and entry-heading angle from Table 1. It is evident from Table 2 that the best trajectory generated with the most area covered is for the discrete turning rate set of 0, 0.23562, -0.23562, 0.09599, -0.09599 rad/s, since it covers 97.71 percent of the region. However, as in the previous case the trajectory is not the ideal trajectory in approaching the exit point, since other generated trajectory get nearer to the exit point at the end of the mission.

Table 3 provides the results of the generated trajectory for the possible combinations of a set of seven turn rates that include the five best turning rates from

Table 2 that covered the most area. It is evident that the discrete turning rate set of 0, 0.23562, -0.23562, 0.09599, -0.09599, .16806, and -.16806 rad/s generates the best trajectory in covering more of the specified region. Tables 1 through 3 demonstrate the amount of iterations required to obtain the discrete set of turning rates that generates an optimal trajectory. More importantly, the results demonstrate that appropriate selection of turn rates leads to optimal performances but are unknown unless performing a simulation of several cases.

TABLE 3. Percent of Area Covered and Distance from Exit Point for a Set of Seven Turning Rates

Turn Rates (rad/s)	Percent Area Covered	Distance from Exit (m)
0.00873, -0.00873	94.74	47.45
0.01745, -0.01745	43.51	74.24
0.02618, -0.02618	88.19	86.52
0.03491, -0.03491	91.79	85.69
0.04363, -0.04363	95.62	69.84
0.05236, -0.05236	90.62	23.45
0.06109, -0.06109	60.31	67.09
0.06981, -0.06981	87.43	97.35
0.07854, -0.07854	94.01	74.10
0.08727, -0.08727	88.13	47.07
0.10472, -0.10472	96.60	85.89
0.11345, -0.11345	94.98	22.97
0.12217, -0.12217	96.35	88.29
0.13090, -0.13090	93.07	90.89
0.13963, -0.13963	93.77	87.24
0.14835, -0.14835	72.18	88.04
0.15708, -0.15708	82.15	39.08
0.16581, -0.16581	98.05	49.69
0.17453, -0.17453	52.33	91.12
0.18326, -0.18326	58.81	84.45
0.19199, -0.19199	85.31	113.04
0.20071, -0.20071	79.96	33.48
0.20944, -0.20944	48.47	10.31
0.21817, -0.21817	82.46	67.37

TABLE 3. Continued Percent and Distance from Exit for a Set of Seven Turning Rates

Turn Rates (rad/s)	Percent Area Covered	Distance from Exit (m)
0.22689, -0.22689	93.41	56.73
0.24435, -0.24435	96.44	79.42
0.25307, -0.25307	85.31	83.10
0.26180, -0.26180	90.39	83.50
0.27053, -0.27053	70.99	20.75
0.27925, -0.27925	62.30	35.90
0.28798, -0.28798	84.59	113.41
0.29671, -0.29671	96.54	33.87
0.30543, -0.30543	96.55	102.56

The table presents the percent of area covered and the distance from the desired exit point for the trajectories generated for a set of seven turning rates. The discrete set of turning rates includes the most optimal five turning rates from Table 2 of 0, 0.23562, -0.23562, 0.09599, and -0.09599 rad/s. The parameters used to generate are the same parameters used for Table 1 and Table 2.

The enormous amount of iterations performed to obtain the discrete set of turning rates that generate the best coverage trajectory is cumbersome. There is no guarantee that the obtained set of turning rates is the best set of turning rates that produces the best trajectory that covers the most area and that approaches the exit point the most. For instance, Figures 5 and 6 illustrate the situation that there exist better sets of turn rates than the obtained set of turning rates. Figure 5 and 6 demonstrate the percent of the region covered and the distance from the exit point for a particular amount of turning rates in the order of the provided discrete set of turning rates. It is evident from Figure 5 that the generated trajectories for the stated set of turning rates converges to 98% coverage of the region for a set seven turn rates. On the other hand, Figure 6 demonstrates that the distance of the vehicle at the end of the mission does not converge for any possible combination of a set of seven turn rates since the distance varies widely for the provided set of turn rates. So the discrete set of turning rates, obtained from

Tables 1 through 3, do not generate the ideal trajectory that will cover the most area and approach closest to the exit point since other combinations of turning rates exist that generate trajectories that will cover the same amount of area but get nearer to the exit point. Even though, the discrete set of turning rates of 0, .23562, -.23562, .09599, -.09599, .165806279, and -.165806279 rad/s provided in Figure 1 and 2 is better than the set of turning rates obtained in Table 3, it does not mean that this particular set of turning rates is the best set of turning rates.

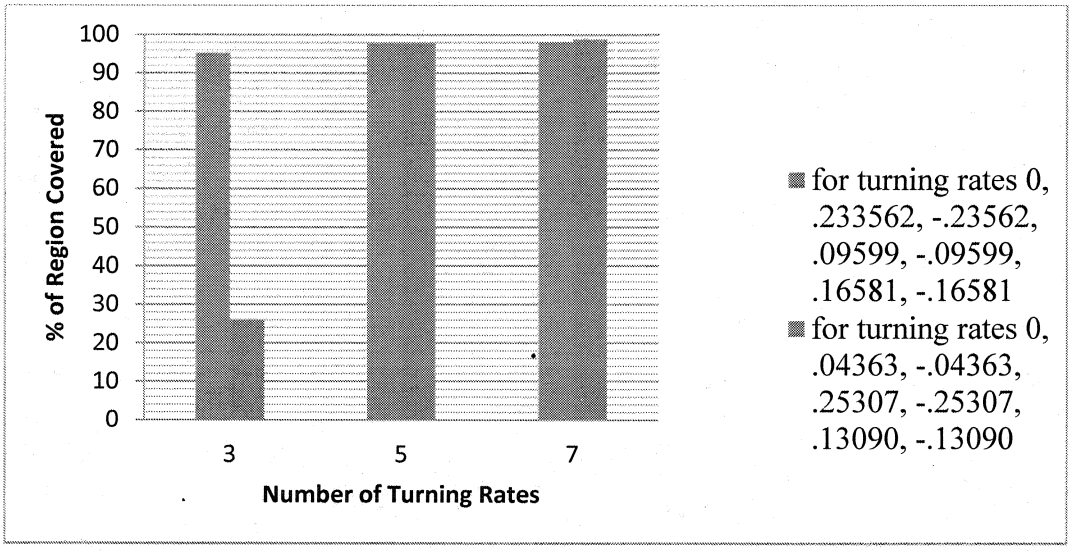

FIGURE 5. Percent covered versus number of turning rates. Figure presents the percent of the region covered versus the number of turn rates used for two discrete sets of turning rates. The order of the two-presented discrete set of turning rates is the order of number of turn rates used to generate the trajectories.

It is apparent that, to obtain the best set of turning rates that produce the absolute best coverage trajectory and gets as near as possible to the exit state for a particular set of conditions, multiple iterations for calculating the trajectory for all the possible turn rate

combinations is necessary, which is very time consuming. Therefore, the existing algorithm is not an ideal algorithm in generating the trajectory that will cover the most area and satisfies the exit state since it requires the operator to make the correct selection of the discrete turning rate set to generate the optimal trajectory. The algorithm's dependence on the operator making the correct selection gives the algorithm a limited autonomy in generating an optimal trajectory.

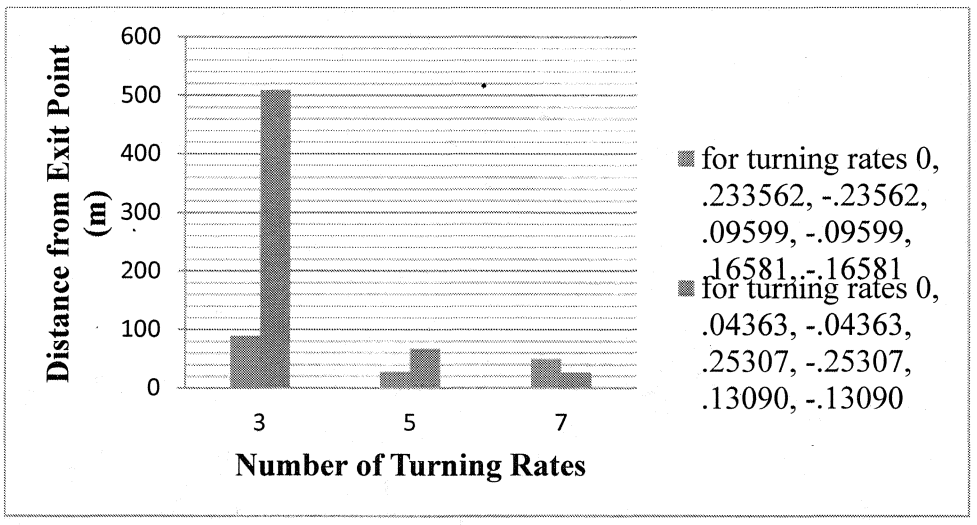

FIGURE 6. Distance from exit point versus number of turning rates. The figure presents the distance of the vehicle at the end of the mission versus the number of turn rates used for two discrete sets of turning rates. The order of the two-presented discrete set of turning rates is the order of number of turn rates used to generate the trajectories.

3.1.2 Effects on Generated Trajectory for Varying Turn Duration

In addition, the existing algorithm generates trajectories that vary greatly in performance of the percent of area covered and the distance from the exit point for different turning duration. The results generated for Table 4 are for an entry heading

angle of 45 degrees, entry point of p^{entry}=[10, 10], and the optimal discrete turning rate set presented in Figure 1 and 2. From Table 4 it is evident that the percent of the area covered and the distance from the exit point varies greatly for different turn duration. Therefore, for the existing algorithm the operator has to select the appropriate turn duration to generate the optimal trajectory for the provided discrete set of turning rates.

TABLE 4. Performance of Trajectories Generated Using RHC Based Algorithm Without the Energy Constraints and Selecting Trajectories for a Discrete Set of Turning Rates for Different Selected Turn Duration

Turn Duration (sec)	Percent Covered	Distance from Exit (m)
2	50.35	18.95
3	60.72	30.97
4	52.52	70.09
5	60.99	56.87
6	74.57	65.04
7	77.32	50.43
8	85.70	47.29
9	83.57	51.52
10	98.80	26.68
11	91.00	57.19
12	88.38	72.92
13	94.38	74.82
14	88.50	93.13
15	88.43	87.06
16	92.11	33.86
17	93.54	56.16
18	89.16	65.04
19	93.07	84.94
20	88.28	18.56
21	89.96	94.49
22	90.67	118.90
23	87.12	553.78
24	87.07	42.49
25	69.75	47.16

The table provides the percent covered and the distance of from the exit point for different turning durations using the existing algorithm presented, for a discrete set of turning rates of 0, .04363, -.04363, .25307, -.25307, .13090, -.13090 rad/s. The parameters of the generated trajectories are an entry point of [10, 10], entry-heading angle of 45 degree, desired exit point of (10,569), and a mission duration of 9 minutes.

3.1.3 Effects on Generated Trajectory for Varying Entry-Heading Angle

Similarly, the existing algorithm requires the operator to provide a particular entry-heading angle that generates an optimal trajectory since the percent of area covered and distance from the exit point vary widely for different entry-heading angles. Results generated for Tables 5 are for a 10-second turn duration, the discrete turning rate set used in Table 4, and the entry point used in the previous tables. Table 5 demonstrates that the generated trajectories result in in a large difference in the percent of area covered and the distance from the exit point for varying the entry-heading angle.

TABLE 5. Performance of Trajectories Generated Using RHC Based Algorithm Without Energy Constraints and Selecting Trajectories from a Discrete Set of Turning Rates for Different Selection of Entry-Heading Angle

Entry-Heading Angle (degrees)	Percent Area Covered	Distance from Exit (m)
0	96.79	96.96
5	94.86	123.03
10	96.02	78.57
15	95.45	60.83
20	94.46	48.64
25	94.71	18.67
30	83.58	71.19
35	96.56	75.29
40	95.33	60.71
45	98.80	26.68
50	96.97	79.25
55	94.75	39.30
60	80.83	66.37
65	87.66	40.53
70	97.82	59.74
75	92.08	36.00
80	96.42	6.94
85	92.39	72.53
90	93.95	89.04

The table presents the percent of area covered and distance from the exit point using the existing algorithm for varying entry-heading angle. The parameters used to generate the trajectories are an entry-heading angle of 45 degrees, entry point of [10, 10], exit point of [10, 569], and mission duration of 9 minutes. The trajectories generated are for the same discrete set of turning rates used in Table 4.

3.1.4 Effects of Entry Point on Generated Trajectory

Furthermore, the selected entry point by the operator also affects the generated trajectory by the existing algorithm. Table 6 provides the results for the generated trajectory with an entry-heading angle of 45 degrees, turn duration of 10 seconds, the discrete set of turning rates pervious used in Tables 4 through 5, and for a varying entry point. Table 6 makes it evident that for the existing algorithm the operator needs to select the appropriate entry point to generate a trajectory that will cover 80% of the specified region.

TABLE 6. Performance of Trajectories Generated Using the RHC Based Algorithm Without the Energy Constraints and Selecting the Trajectory from a Discrete Set of Turning Rates for Varying Entry Points

Entry Point	Percent Covered	Distance from Exit (m)
[10,10]	98.80	26.68
[10, 72.11]	97.45	76.32
[10, 134.22]	95.95	33.90
[10, 196.33]	97.11	85.63
[10, 258.44]	78.28	53.18
[10, 320.56]	96.52	87.08
[10, 382.67]	87.17	70.29
[10, 444.78]	76.15	81.83
[10, 506.89]	94.24	4.78
[10, 569]	95.02	57.19

The table provides the percent of area covered and distance using the existing algorithm for the provided entry points. The parameters used to generate the trajectories are a 10 second turn duration, entry-heading angle of 45 degrees, exit point [10, 569], and a 9 minute mission duration. The trajectories generated are for the same discrete set of turning rates used in Table 4.

From the results presented in Tables 1 through 6 it is evident that the existing algorithm has a limited autonomy in generating the optimal trajectory that maximizes the

spatial-temporal coverage while still satisfying the original flight plan of reaching the exit point at the end of the mission. The existing algorithm depends on the operator providing the correct combination of discrete set of turning rates, turn duration, entry-heading angle, and entry point to generate the optimal trajectory that maximizes the area covered and approaches the desired exit point the most at the end of the mission.

3.2 Simulation Results of Modified Algorithm

This section presents the simulation results of the proposed modified algorithm, which should increase the autonomy of the algorithm in generating the most optimal trajectory possible for any selected conditions. The results presented of the modified algorithm are for varying turn duration, entry-heading angle, and entry point. This section compares the results of the modified algorithm with that of the receding horizon control based algorithm without the energy constraint and a discrete set of turning rates in order to verify if the proposed algorithm improves the performance of the existing algorithm. The bounds of the range of turning rates are -6283 and .6283 rad/s.

3.2.1 Effects on Generated Trajectory for Varying Turn Duration

Table 7 provides the results of the generated trajectory using the modified algorithm for varying turn duration. The generated trajectories in Table 7 are for a range of turning rates instead of a discrete set of turning rates, in which the bound of the turning rate range is -.6283 and .6283 rad/s. The trajectories generated are for an entry heading angle of 45 degrees, and entry point p^{entry}=[10, 10]. Comparing Table 4 to Table 7 it is evident that the modified algorithm generates trajectories with high percent of area covered. In addition, from comparing the two tables the modified algorithm on average

generates trajectories that approach the desired exit point more than the existing algorithm. For instance, the greatest distance from the desired exit point produced by the modified algorithm is 91.91 meters, while for the existing algorithm the largest distance from the desired exit point is 118.90 meters.

TABLE 7. Performance of Generated Trajectories Using RHC Based Algorithm Without Energy Constraints and Selecting the Trajectory from a Range of Turning Rates for Varying Turn Duration

Turn Duration (sec)	Percent Area Covered	Distance from Exit Point (m)
2	98.56	9.82
3	96.56	1.61
4	94.81	7.16
5	92.92	4.89
6	98.96	31.15
7	90.74	8.49
8	99.58	16.14
9	97.73	32.59
10	91.05	26.06
11	94.16	10.95
12	96.21	68.04
13	95.52	65.24
14	97.69	59.49
15	96.51	38.03
16	90.39	91.91
17	88.73	61.57
18	93.79	85.29
19	93.70	63.40
20	97.70	54.42
21	90.50	57.66
22	94.98	21.04
23	94.82	90.17
24	94.75	41.52
25	90.59	30.18

The table provides the percent of area covered and the distance from the exit point for the trajectories generated using the developed algorithm for varying turn duration. The algorithm optimized the generated trajectories for a range of turning rates bounded by -.6283 and .6283 rad/s. The parameters used to generate the trajectories are entry-heading

angle of 45 degrees, entry point of [10, 10], exit point [10, 569], and mission duration of 9 minutes.

The modified algorithm generates trajectories that also approach the desired exit point more than the trajectories generated by the existing algorithm, since the modified algorithm generates a trajectory that ends 1.61 meters from exit point and the closest generated end of trajectory for the existing algorithm is 18.56 meters. The modified algorithm performs its task of generating trajectories with a higher average of percent of area covered and lower average of distance from the end of the trajectory to the desired exit point for trajectories generated for any selected value of turn duration.

3.2.2 Effects on Generated Trajectory for Varying Entry-Heading Angle

Table 8 provides the generated trajectories using the modified algorithm for the same range of turning rates defined for Table 7, turn duration of 10 seconds, entry point p^{entry}=[10,10], and varying entry-heading angles. The rest of the parameters are the same for the generated trajectories in Table 7. Comparing Table 5 and 8 it is evident that the modified algorithm improves the performance of the existing algorithm by increasing the autonomy of the algorithm in generating adequate optimal trajectories, in which the selection of the variables does not significantly degrade the percentage of area covered or increase the distance from the exit point. The modified algorithm on average generates trajectory with a higher percent of area covered and lower distance from the end of the trajectory to the desired exit point than the existing algorithm. Even though, some of the trajectories in Table 5 may have a slightly better performance than a trajectory in Table 8 for the same entry-heading angle, the modified algorithm guarantees that for mostly any selected entry-heading angle the generated trajectory will perform better than the existing

algorithm. In addition, as previously mentioned the trajectories generated in Table 5 has the added complexity of the operator selecting the correct discrete set of turning rates, which is an issue that the operator does not have to deal with for the generated trajectories of the modified algorithm presented in Table 8.

TABLE 8. Performance of Trajectories Generated Using the RHC Algorithm Without Energy Constraints and Selecting the Trajectory from a Range of Turning Rates for Varying Entry-Heading Angle

Entry-Heading Angle (deg)	Percent Area Covered	Distance from Exit Point (m)
0	96.70	7.33
5	96.61	15.43
10	92.22	11.93
15	95.39	29.30
20	98.06	12.25
25	96.05	40.83
30	96.45	52.88
35	98.05	12.94
40	86.92	15.59
45	91.05	26.06
50	91.53	20.79
55	97.06	18.90
60	96.65	12.39
65	95.94	25.22
70	91.13	39.50
75	96.90	55.51
80	97.24	23.70
85	95.52	28.04
90	96.72	8.10

The table provides the percent of area covered and the distance from the exist point of the generated trajectories for varying entry heading angle using the developed algorithm. The algorithm optimizes the generated trajectories for a range of turning rates bounded by the turning rates of -.6283 and .6283 rad/s. The parameters used to generate the trajectories are a10-second turn duration, exit point of [10, 569], entry point of [10, 10], and mission duration of 9 minutes.

3.2.3 Effects on Generated Trajectory for Varying Entry Point

Lastly, Table 9 provides the generated trajectories using the modified algorithm and using the same parameters as Table 6 but optimizing the trajectory for a range of

turning rates bounded by the rate that produces a 360-degree turn for the 10-second turn duration. By comparing Table 9 and Table 6, it is evident that the modified algorithm does perform better since on average it generates trajectories that have a higher percent of area covered and lower distance from the end of the trajectory to the desired exit point for any selected entry point. Even though, some of the generated trajectories in Table 6 perform slightly better than trajectories in Table 9 for the same entry point, the modified algorithm eliminates the requirement of selecting the correct combination of turning rates. The slightly better performance of the generated trajectories in Table 6 than in Table 9 for the same entry point does not merit using the existing algorithm, since existing algorithm produces very poor coverage for the wrong selection of the entry point.

TABLE 9. Performance of Generated Trajectories Using the RHC Algorithm Without the Energy Constraints and Selecting the Trajectory from a Range of Turning Rates for Varying Entry Point

Entry Point	Percent Area Covered	Distance from Exit (m)
[10, 10]	91.05	26.06
[10, 72.11]	96.53	13.14
[10, 134.22]	91.15	32.82
[10, 196.33]	92.11	25.08
[10, 258.44]	99.20	33.07
[10, 320.56]	97.76	14.88
[10, 382.67]	95.44	6.71
[10, 444.78]	97.08	24.63
[10, 506.89]	90.79	17.21
[10, 569]	93.92	38.09

The table provides the percent of area covered and the distance from the exit point for the generated trajectories using the developed algorithm for varying entry points. The algorithm optimizes the generated trajectories for a range of turning rates bounded by the turning rates of -.6283 and .6283 rad/s. The parameters used to generate the trajectories area a 10-second turn duration, exit point o f [10,569], entry-heading angle of 45 degrees, entry point of [10, 10], and mission duration of 9 minutes.

The results demonstrated that the modified algorithm does have an increased autonomy in generating the optimal trajectory since on average for the three variables the algorithm generates trajectories with higher percent of area covered and lower distance from the end of the trajectory to the desired exit point. More importantly, the higher average of percent of area covered and lower average of distance from the end of the trajectory to the desired point eliminated the dependency of the algorithm on the operator providing the correct values that did not generated trajectories highly degraded from the most optimal trajectory. The increased autonomy enables the algorithm to generate near optimal trajectories for any selected condition.

3.3 Simulation Results of Algorithm with Energy Constraints and Maneuverability Limitations

This section presents the results for the developed algorithm that considers the energy constraint to optimize the coverage trajectory and still maintain the original flight plan of reaching the desired exit point at the end of the mission. The algorithm optimizes the trajectory for the energy constraint by calculating the amount of energy consumed by the vehicle to perform a particular maneuver and comparing the remaining energy after completing the maneuver to the energy required to reach the desired exit point. If enough energy remains after a maneuver to reach the desired point exit point then the algorithm selects the path that covers more area. However, as the amount of energy remaining reduces the objective of the algorithm switches to select the path that directs the vehicle to the desired exit point requiring the least amount of energy consumption.

This section describes the performance results of the trajectories generated for the energy constraint with the performance results of a vehicle with energy constraints

performing the trajectories generated for the time constraint instead of an energy constraint. The trajectories generated for the energy constraint optimize the trajectory so that it covers the most area possible and satisfy the exit point for the energy available. The trajectories generated for the time constraint optimize the trajectory so that the trajectory covers the most area possible and satisfy the exit point for the mission time duration. The results include the performance of a vehicle with energy constraint performing the generated trajectories without the energy constraint in order to evaluate the effectiveness of optimizing the trajectory for the energy available. The results compare the two scenarios for varying turn duration, entry-heading angle, and entry point.

3.3.1 Comparison of Varying Turn Duration

Table 10 and 11 are the performance results for the generated trajectory with energy constraint and the actual performance of a vehicle with energy constraint performing a trajectory generated without the energy constraint for varying turn duration. The generated results are for the parameters of an entry-heading angle of 45 degrees and an entry point $p^{entry}=[10, 10]$. It is evident when comparing the two tables that the generated trajectories with energy constraint are more optimal since on average the trajectories considering the energy constraint result in a smaller distance from the end of the trajectory to the desired exit point than the trajectories without the energy constraint. The results from Table 11 indicate that a vehicle using trajectories not optimized for the energy constraint on average ends the mission at a greater distance from the exit state that the trajectories optimized for the energy constraint since the vehicle consumes the energy

before approaching the exit point. The vehicle consumes the energy before the energy constraint because it is using a trajectory not optimized for the energy available.

TABLE 10. Performance Results for Trajectories Generated Using the RHC Algorithm with Energy Constraints and Range of Turning Rates for Varying Turn Duration

Turn Duration (s)	Percent Area Covered	Distance from Exit (m)	Flight Time (s)
2	93.32	25.84	470
3	91.62	25.09	489
4	94.35	35.54	492
5	95.65	28.58	495
6	99.00	60.53	498
7	97.31	30.66	504
8	98.13	76.67	496
9	90.59	74.98	495
10	93.68	76.41	500
11	93.94	41.75	495
12	96.77	82.28	504
13	95.40	72.78	507
14	92.70	31.25	504
15	89.37	147.53	495
16	90.49	161.18	496
17	91.03	98.68	493
18	91.18	47.63	504
19	86.43	170.35	494
20	94.81	106.22	500
21	92.39	41.41	504
22	94.47	142.56	506
23	85.23	187.02	483
24	77.96	132.53	504
25	85.43	212.35	475

The table presents the percent of area covered, distance from the exit point, and flight time of the generated trajectories using the developed algorithm for varying turn duration. The parameters used to generate the trajectories are entry-heading angle of 45 degrees, entry point of [10, 10], exit point of [10, 569], total energy of 87912 Joules, and turning rate range bounded by -.9548 and .9548 rad/s.

TABLE 11. Performance Results of a Vehicle with Energy Limitations Performing a Trajectory Generated with the RHC Algorithm Without Energy Constraints and Range of Turning Rates for Varying Turn Duration

Turn Duration (sec)	Percent Covered	Distance from Exit	Flight time (sec)
2	94.83	156.79	468
3	96.22	396.45	471
4	94.40	71.10	488
5	94.37	235.84	490
6	99.00	6.57	492
7	97.87	207.27	504
8	98.13	253.69	496
9	85.89	258.70	486
10	96.73	288.55	500
11	93.79	302.07	484
12	97.45	207.51	504
13	95.92	262.48	494
14	93.63	213.57	504
15	90.21	255.59	495
16	90.00	253.81	496
17	90.92	259.35	493
18	84.45	316.18	486
19	86.43	270.25	494
20	94.38	218.51	500
21	92.16	374.89	483
22	92.97	323.75	484
23	85.23	224.53	483
24	78.75	391.19	480
25	88.35	468.71	475

The table presents percent of area covered, distance from exit point, and flight time performance of a vehicle with limited energy performing a trajectory not optimized for the energy constraint turn duration. The parameters used to generate the trajectory are entry point of [10, 10], exit point of [10, 569], entry-heading angle of 45 degrees, mission duration time of 9 minutes, vehicle with a total energy of 87912 Joules, and turning rate range bounded by -.9548 and .9548 rad/s.

Figure 7 demonstrates the distance results from Table 10 and 11. Figure 7 demonstrates the conclusion previously stated that the trajectories generated with the energy constraint on average end nearer to the desired exit state than the trajectories

generated without the energy constraint. As previously stated, the algorithm considering the energy constraint provides some assurance that the vehicle will end closer to the exit state, which is important when retrieving the vehicle. The algorithm that does not optimize the trajectory for the energy constraint makes it difficult to recover the vehicle since the point at which the vehicle ends the mission is uncertain.

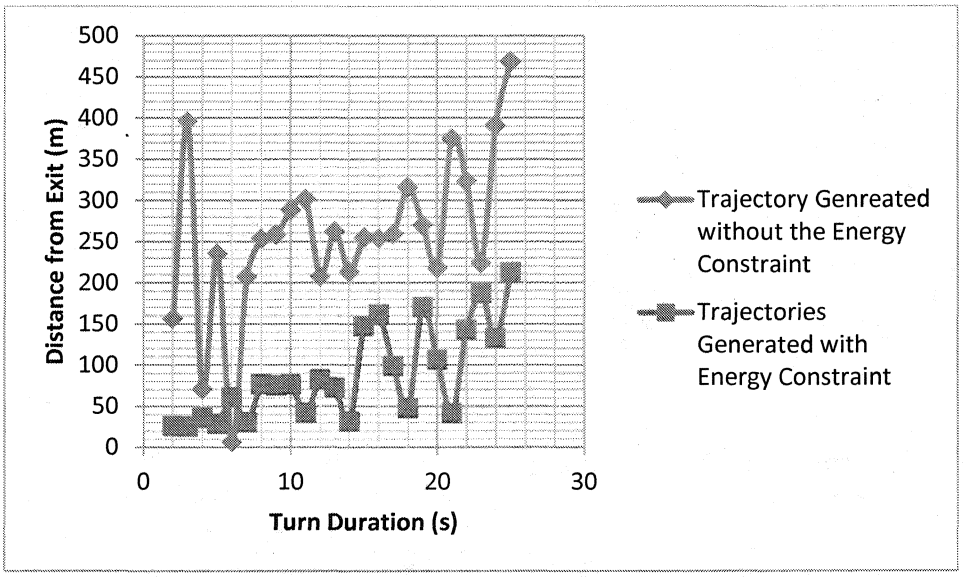

FIGURE 7. Distance from exit versus turn duration. The figure presents the distance of the vehicle at the end of mission for the two cases discussed.

3.3.2 Comparison of Varying Entry-Heading Angle

Table 12 and 13 are the performance result of the generated trajectories with energy constraint and a vehicle with limited energy executing a trajectory not optimized for the energy constraint for varying entry-heading angle, respectively. The generated performance results for Table 12 and 13 are for the same parameters with the exception of the fixed turn duration of 10 seconds. Comparing the performance of the trajectories,

it is evident that on average both approaches cover about the same percentage of the specified region. Both approaches of optimizing the trajectory on average also cover the same amount of area for the same amount of flight time. However, comparing the distance of the vehicle from the exit state when the vehicle consumes all the available energy for the two cases provides a useful method to evaluate the effectiveness of both approaches.

TABLE 12. Performance Results of Trajectories Generated Using RHC Algorithm with Energy Constraints and Range of Turning for Varying Entry-Heading Angle

Entry-Heading Angle (deg)	Percent Covered	Distance from Exit (m)	Flight Time (s)
0	91.00	77.97	500
5	95.85	59.70	500
10	91.37	132.29	500
15	92.23	139.29	500
20	98.16	163.48	500
25	93.10	188.99	500
30	97.26	100.05	500
35	91.39	80.94	500
40	97.20	153.88	500
45	93.68	76.41	500
50	89.74	103.51	500
55	93.73	95.84	490
60	95.19	50.19	490
65	98.55	106.52	500
70	98.16	53.46	510
75	92.20	24.66	500
80	94.06	62.15	500
85	89.06	116.83	510
90	95.22	62.16	500

The table presents the percent of area covered, distance from the exit point, and flight time of the generated trajectories using the developed algorithm for entry-heading angle. The parameters used to generate the trajectories are a10 second turn duration, entry point of [10, 10], exit point of [10, 569], total energy of 87912 Joules, and turning rate range bounded by -.9548 and .9548 rad/s.

TABLE 13. Performance Results for a Vehicle with Energy Limitations Performing a Trajectory Generated Using RHC Algorithm with a Range of Turing Rates and Without the Energy Constraints for Varying Entry-Heading Angle

Entry-Heading Angle (deg)	Percent Covered	Distance from Exit	Flight Time (sec)
0	90.55	291.49	490.00
5	96.68	71.37	500.00
10	91.46	230.59	500.00
15	92.24	255.96	500.00
20	96.06	144.03	500.00
25	93.69	287.87	500.00
30	95.25	204.75	500.00
35	95.38	309.10	490.00
40	97.27	208.65	510.00
45	96.73	288.55	500.00
50	90.96	260.07	500.00
55	96.36	144.17	490.00
60	94.30	312.31	490.00
65	98.70	228.16	500.00
70	98.79	84.07	510.00
75	90.74	230.69	500.00
80	93.00	290.49	500.00
85	89.11	281.66	500.00
90	99.10	230.19	500.00

The table presents percent of area covered, distance from exit point, and flight time performance of a vehicle with limited energy performing a trajectory not optimized for the energy constraint for varying entry angle. The parameters used to generate the trajectory are a 10 second turn duration, entry point of [10, 10], exit point of [10, 569], mission duration time of 9 minutes, vehicle with a total energy of 87912 Joules, and turning rate range bounded by -.9548 and .9548 rad/s.

The distance of the vehicle to the exit point when runs out of energy is the only result considered since, as previously state, the percent covered on average is about the same for both cases and no definitive conclusion results from comparing the percent of area covered. Juxtaposing the distance of the vehicle to the desire exit point for both cases provides a definitive conclusion that is more effective to optimize the trajectory for

the energy constraint. The results demonstrate that optimizing the trajectory for the energy constraint on average cover the same amount of area and approach the exit point the most. The trend that distance of the vehicle from the exit point on average is smaller is evident in Figure 8. Optimization of the trajectory for the energy constraint guarantees that the vehicle reaches the desired exit point more than a trajectory not optimized for the energy constraint since using the trajectory optimized for the energy ensures that the vehicle runs out of energy near the exit point. The optimization of the trajectory for the time constraint instead of the energy constraint makes the location at which the vehicle runs out of energy high uncertain, which does not ensure that the vehicle runs out of energy near the exit state.

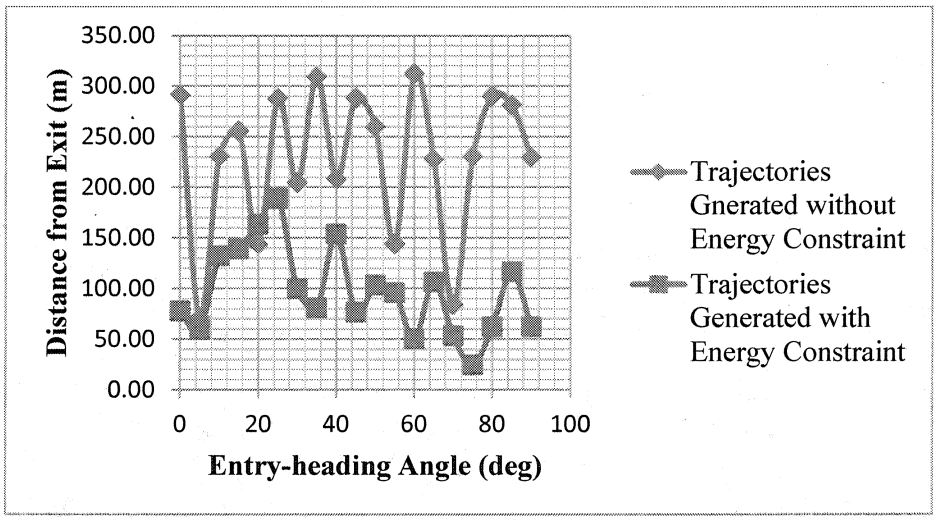

FIGURE 8. Distance from exit versus entry-heading angle. The figure presents the distance from the exit point for the both cases discusses and provides in Tables 12 and 13.

3.3.3 Comparison of Varying Entry Points

Tables 14 and 15 provide the performance result of the generated trajectory considering the energy constraint and of a vehicle, with energy constraint s, executing the generated trajectory that does not consider the energy constraint for varying entry points, respectively. The generated performance results for both tables are for the same parameters from Tables 12 and 13 with the exception of a fixed entry-heading angle of 45 degrees. It is evident from Table 12 that the generated trajectory with the energy constraint is more efficient than the trajectories generated without the energy constraint, since on average both method cover about the same percent of the specified region but the trajectories generated with the energy constraint on average result in the trajectories finishing nearer to the desired exit point. The trajectories in Table 12 are trajectories optimized for the available energy, which guarantees that the trajectory will approach the desired exit point for the energy available. However, the trajectories in Table 15 are trajectories not optimized for the available energy of the vehicle as it performs the mission, resulting in the vehicle consuming the total available energy before completing the planned path and incapable of reaching the desired exit point. Figure 9 demonstrates the results visually making it easier to arrive to the conclusion that the trajectories generated with the energy constraint end nearer to the exit state. As previously stated, optimizing the trajectory for the available energy of the vehicle as it performs the mission directs the vehicle along a path that enables the vehicle to complete its task of maximizing the coverage of the specified region and to reach the desired exit point for

the total available energy. Otherwise, the vehicle runs out of energy at a point far away from the desired exit point as it occurred in the results of Table 15.

TABLE 14. Performance Results of Trajectories Generated Using RHC Algorithm with Range of Turing Rates and Energy Constraints for Varying Entry Point

Entry Point	Percent Covered	Distance from Exit (m)	Flight Time (sec)
[10, 10]	93.68101014	76.40602213	500
[10, 72.11]	96.8438728	129.3438868	500
[10, 134.42]	95.61201313	88.21706874	490
[10, 196.33]	93.24926034	137.8242588	500
[10, 258.44]	96.61509616	60.76051496	510
[10, 320.56]	96.31974881	136.0141892	500
[10, 382.67]	93.53223061	138.8199157	490
[10, 444.78]	93.21447579	197.7827994	490
[10, 506.89]	95.79663284	43.27921609	510
[10, 569]	91.94642482	83.30219797	490

The table presents the percent of area covered, distance from the exit point, and flight time of the generated trajectories using the developed algorithm for varying entry point. The parameters used to generate the trajectories are a10 second turn duration, entry-heading angle of 45 degrees, exit point of [10, 569], total energy of 87912 Joules, and turning rate range bounded by -.9548 and .9548 rad/s.

TABLE 15. Performance Results of a Vehicle with Energy Limitations Performing Trajectories Generated with the RHC Algorithm with Range of Turning Rates but No Energy Constraints for Varying Entry Point

Entry point	Percent Covered	Distance from Exit (m)	Flight Time (sec)
[10, 10]	96.73	288.55	500
[10, 72.11]	96.98	237.35	500
[10, 134.42]	96.11	287.61	490
[10, 196.33]	93.28	288.75	500
[10, 258.44]	96.62	261.90	500
[10, 320.56]	97.63	231.16	510
[10, 382.67]	95.11	346.52	490
[10, 444.78]	93.92	287.00	490
[10, 506.89]	95.81	285.64	500
[10, 569]	92.79	287.80	490

The table presents percent of area covered, distance from exit point, and flight time performance of a vehicle with limited energy performing a trajectory not optimized for the energy constraint for varying entry point. The parameters used to generate the trajectory are a 10 second turn duration, exit point of [10, 569], entry-heading angle of 45 degrees, total energy of 87912 Joules, and turning rate range bounded by -.9548 and .9548 rad/s.

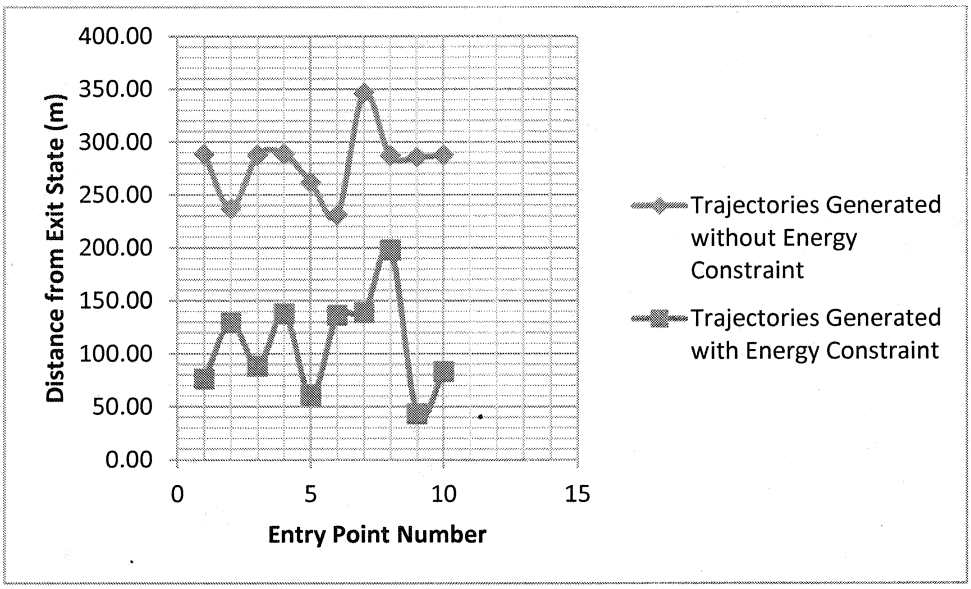

FIGURE 9. Distance from exit versus entry point. The figure present the distance result for both cases presented in Tables 14 and 15.

Figure 10 demonstrates the vehicle's trajectory generated with the energy constraint for a particular set of conditions. The parameters for the generated trajectory demonstrated in figure 6 are turn duration of 3 seconds, entry point of [10 10], exit point of [10 569], velocity of 11.49 m/s, and a range bounded by -.9546 and .9546 rad/s. In addition, the vehicle has a total energy at the beginning of the mission of 87912 Joules for a battery with 2200 mAh and 11.1 volts. The figure demonstrates that the vehicle selects a trajectory that covers as much area possible and still attempts to satisfy the exit constraint of reaching the desired exit state. Even though, it does not completely reach the exit state the trajectory does better job than the current algorithm that does not consider the energy constraint in generating the trajectory.

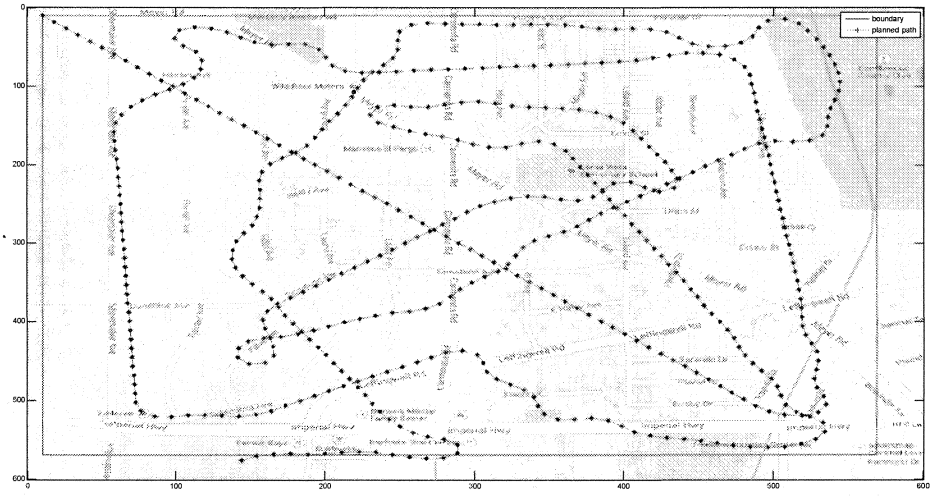

FIGURE 10. Trajectory generated utilizing the developed RHC algorithm optimizing the trajectory for range of turn rates and energy constraint.

The results demonstrated that the trajectories generated with the energy constraint perform better since on average the algorithm produce trajectories that results in the trajectories finishing nearer to the desired exit point and covering the same amount of area as the trajectories generated without the energy constraint. The trajectories generated without the energy constraint assumes that the energy consumption of the vehicle is constant, which is not realistic since the energy consumption varies for different maneuvers. However, the trajectories generated with the energy constraint consider the varying energy consumption of the vehicle for different maneuvers and the remaining energy as the vehicle performs the mission, providing the algorithm more comprehensive information so that it selects the most optimal trajectory for the energy available. The assumption that the energy consumption is constant for the trajectory

generated without the energy constraints is the reason that a vehicle with limited power runs out of energy far from the desired point. The vehicle consumes the total energy faster since in reality the power consumption is not constant. More importantly, the results prove that the trajectories optimized for the available energy is a more effective method of generating the trajectory since it is certain that the vehicle approaches the desired exit point for the available energy. On the other hand, the trajectory optimization for a mission duration constraint instead of the energy constraint does not ensure that the vehicle finish the mission for near the exit point for the energy available, making the location at which the vehicle runs out of energy uncertain.

CHAPTER 4

CONCLUSION

The results demonstrate that the proposed algorithm increases the autonomy of the algorithm in generating the optimal trajectory for a search and coverage mission in which the trajectory has to satisfy the initial flight plan of reaching the desired exit point at the end of the mission. The existing algorithm relies on the operator providing the correct combination of discrete turning rates, turn duration, entry heading angle, and entry point in generating an optimal trajectory that maximizes percentage of the area covered and end the mission as near as possible to the exit state. However, the presented algorithm does not require the operator providing any specific condition since it optimizes the trajectory for any selected conditions, providing trajectory with near optimal coverage of the specified region for any selected value. In addition, the developed algorithm does not rely on a discrete set of turning rates since it optimizes the trajectory for a range of turning rates, removing the human factor in generating the optimal trajectory since the selection of the discrete set of turning rates has an influence in the trajectory generated.

Moreover, the developed algorithm generates better trajectories since it considers the energy constraint of the vehicle in generating the optimal trajectory. The existing algorithm optimized the trajectory that covers the most area and reaches the exit point for an allocated mission time. The allocated mission time is the endurance of the vehicle for

the energy available that assumes constant energy consumption. So optimizing the trajectory for the allocated mission time assumes the energy consumption of the vehicle is constant which is impractical since in reality the energy consumption is not constant. The energy is not constant since the mission requires maneuvers and energy consumption varies for different maneuvers.

Generating the trajectory without the energy does not ensure that the vehicle reaches the exit state since the optimization of the trajectory is so that the vehicle reaches the exit point at the end of the allocated mission duration time, which assumes constant energy consumption. However, as previously stated, the vehicle does not consume energy at a constant rate since it has to perform maneuverers throughout the mission that causes the energy consumption to vary. The varying energy consumption leads to the vehicle consuming the total energy available before the allocated mission duration time, which means that the allocated mission duration time is not the actual duration of the mission. The proposed algorithm generates a trajectory for the actual mission duration since it optimizes the trajectory for the energy constraint providing the time it takes the vehicle to consume the total energy available at the beginning of the mission, which is the time the vehicle ends the mission. More importantly, the optimization leads to a trajectory that covers about the same percentage of the specified region in less time than the allocated mission duration time, the vehicle's endurance.

In addition, optimizing the trajectory for the energy constraint makes easier to recover the vehicle at the end of the mission. The generated trajectory with the energy constraint makes it easier to recover the vehicle since it makes the vehicle approach the

exit point as much as possible for the energy available. The fact that the vehicle approaches the exit point as much as possible for the exit point provides some certainty to the operator of the location to search for the vehicle at the end of the mission. However, generating the trajectory without the energy constraint makes the recovery of the vehicle difficult since the location of the vehicle when it ran out of energy is uncertain. The location of the vehicle is uncertain since the generated trajectory without the energy constraint optimizes the trajectory so that it reaches the exit point at the end of the allocated mission duration time and as previously stated the vehicle consumes the total energy before the allocated mission duration time. The vehicle consuming the total energy available before the allocated mission duration means that the vehicle can run out of energy at a point that is not near the desired exit state when performing a trajectory optimized for the mission duration.

Overall, the proposed algorithm performs as desired. The algorithm has an increased autonomy since it does not depend on the operator making the appropriate selection of conditions or set of turning rates and generates the most optimal trajectory for any conditions. The algorithm with energy constraint is definitely the most effective way of generating the trajectory since it covers about the same amount of area as the trajectory with the time constraint. Ultimately, the trajectory generated with the energy constraint ensures that the vehicle ends the mission near the exit point and not left stranded far from the exit point.

4.1 Future Work

While this thesis demonstrated the efficiency of generating an optimal trajectory that covers the most area possible and satisfies the exit state with a high autonomy algorithm that considers the energy constraint of a vehicle, many opportunities of extending the scope of this thesis remain. This section discusses some of the possible directions of future work.

The current model of the energy consumption of the vehicle does not include the electrical energy consumption of the vehicle. The electrical energy is the energy that the computer, actuators, and other components of the vehicle consume as it performs the mission. Including the electrical energy in the energy consumption model provides a more comprehensive model of the vehicle. The interest in including the electrical energy in the energy consumption is to investigate how the model affects the trajectory generated.

A major limitation of small-unmanned aerial vehicles is the on-board energy capacity that limits the endurance and range of the vehicle. Jack Langelaan's area of interest of optimizing the trajectory so that it extracts energy from the environment, increasing the vehicle's flight time and extending the vehicle's range, is a possible direction to explore [18] [19]. Langelaan's work has proven effective in increasing the vehicle flight time and extending the vehicle's range. Incorporating Langelaan's algorithm to the work presented in this thesis can be effective in generating the trajectory that increases the amount of area that the vehicle can cover during a mission while satisfying the exit state.

REFERENCES

REFERENCES

[1] Ryan, A., Zennaro, M., Howell, A., Sengupta, R., and Hendrikc, J.K., 2004, "An Overview of Emerging Results in Cooperative UAV Control," Proc. IEEE Conference on Decision and Control, IEEE, Nassau, pp. 602-607.

[2] Ryan, A. and Hendrick, J.K., 2005, "A Mode-Switching Path Planner for UAV-Assisted Search and Rescue," Proc. IEEE Conference on Decision and Control, IEEE, Seville, pp. 1471-1476.

[3] Rocha, P. and Gomez, M. A., 2008, "A Decomposition Approach for the Complete Coverage Path Planning Problem," Technical Report, INESCPorto, Faculdade de Engenharia, Universidade Do Porto, Porto.

[4] Choset, H. and Pigno, P., 1998, "Coverage Path Planning: The Boustrophedon Decomposition," Proc. International Conference on Field And Service Robotics, Springer, London, pp. 203-209.

[5] Nourani-Vatani, N., 2007, "Environment, Coverage Algorithms for Under-Actuated Car-like Vehicle in an Uncertain," Proc. IEEE International Conference on Robotics and Automation, IEEE, Roma, pp. 698-703.

[6] Eaungpulswat, P., 2012, "Area Coverage Algorithms for Multiagent Surveillance Task," M.S. Thesis, Technische Universitat Hamburg-Harburg, Hamburg.

[7] Maza, I. and Ollero, A., 2007, "Multiple UAV Cooperative Searching Operation Using Polygon Area Decomposition and Efficient Coverage Algorithms," Distributed Autonomous Robotic systems 6, Springer, Japan, pp. 221-230.

[8] Gillen, D. P., 2002,"Cooperative Behavior Schemes for Improving the Effectiveness of Autonomous Wide Area Search Munitions," Cooperative Control an Optimization, Springer, Ohio, pp. 95-120.

[9] Caves, A. D. J., 2010, "Human-Automation Collaborative RRT For UAV Mission Path Planning," M.S. Thesis, Massachusetts Institute of Technology, Boston.

[10] Balakrishnan, M., 2005, "Coverage Path Planning and Control for Autonomous Mobile Robots," M.S. Thesis, University of Central Florida, Orlando.

[11] Kim, J. S. and Kim, B. K., 2010, "Minimum-Time Grid Coverage Trajectory Planning Algorithm for Mobile Robots with Battery Voltage Constraints," Proc. International Conference on Control, Automation and Systems, IEEE, Gyeonggi-do, pp. 1712-1717.

[12] Waharte, S. and Trigoni, N., 2010, "Supporting Search and Rescue Operations with UAVs," in International Conference on Emerging Security Technologies, Canterbury, pp. 142-147.

[13] Waharte, S., Symington, A., and Trigoni, N., 2010, "Probabilistic Search with Agile UAVs," Proc. IEEE International Conference on Robotics and Automation, Anchorage, pp. 2840-2845.

[14] Polycarpous, M. M., Yang, Y., and Passino K. M., 2001, "Cooperative Control of Distributed Multi-Agent Systems," IEEE Control Systems Magazine, p. 27.

[15] V. Kumar, 2006,"Cooperative Control of UAVs for Search and Coverage," Proc. AUVSI Conference on Unmanned Systems, pp. 1-14.

[16] Raymer, D. P., 2006, Aircraft Design: A Conceptual Approach Fourth Edition, Reston, Virginia: American Institute of Aeronautics and Astronautics Inc.

[17] Anderson, J. D., 2005, Introduction to Flight, New York, New York: McGraw-Hill.

[18] Langelaan, J. W., 2009, "Gust Energy Extraction for Mini and Micro Uninhabited Aerial Vehicles," Journal of Guidance, Control, and Dynamics, vol 32, no. 2, AIAA, pp. 464-473.

[19] Langelaan, J. W., 2007, "Long Distance/Duration Trajectory Optimization for Small UAVs," Proc. Guidance, Navigation, and Control Conference, AIAA, Hilton Head, pp 1-14.